Molecular dynamics study of thermal phenomena in an ultrathin liquid film sheared between solid surfaces: The influence of the crystal plane on energy and momentum transfer at solid-liquid interfaces

Molecular dynamics study of thermal phenomena in an ultrathin liquid film sheared between solid surfaces: The influence of the crystal plane on energy and momentum transfer at solid-liquid interfaces

Taku Ohara[a] and Daichi Torii
Institute of Fluid Science, Tohoku University, 2-1-1 Katahira, Aoba-ku, Sendai, 980-8577, Japan

(Received 19 January 2005; accepted 14 March 2005; published online 7 June 2005)

A molecular dynamics study has been performed on a liquid film sheared between moving solid walls. Thermal phenomena that occur in the Couette-like flow were examined, including energy conversion from macroscopic flow energy to thermal energy, i.e., viscous heating in the macroscopic sense, and heat conduction from the liquid film to the solid wall via liquid-solid interfaces. Four types of crystal planes of fcc lattice were assumed for the surface of the solid wall. The jumps in velocity and temperature at the interface resulting from deteriorated transfer characteristics of thermal energy and momentum at the interface were observed. It was found that the transfer characteristics of thermal energy and momentum at the interfaces are greatly influenced by the types of crystal plane of the solid wall surface which contacts the liquid film. The mechanism by which such a molecular scale structure influences the energy transfer at the interface was examined by analyzing the molecular motion and its contribution to energy transfer at the solid-liquid interface. © *2005 American Institute of Physics*. [DOI: 10.1063/1.1902950]

I. INTRODUCTION

In a liquid film sheared between solid walls, Couette-like macroscopic flow is generated, and the flow energy is converted to thermal energy resulting in an increase in film temperature, which is viscous heating in the macroscopic sense. The thermal energy so generated is transferred via heat flux from the middle of the liquid film to the solid walls on both sides of the film. Such a phenomenon is extremely complicated when the film thickness is of the order of nanometers, because of additional factors such as influences of the solid walls and the large shear rate. Analysis of these phenomena to clarify the characteristics of the thermal energy transfer and momentum transfer is important not only for basic research on nonequilibrium microscopic thermal and fluid phenomena, but also for practical applications, such as lubrication control under extreme conditions, fabrication of low friction surfaces, and the development of new lubricants. For example, a lubricant liquid with a thickness of 1.5–2 nm is coated on a surface of a magnetic hard disk, which rotates over 10 000 rpm. The peripheral velocity near its outer rim reaches 50–100 m/s. The shearing phenomena of such liquid film when the magnetic head gets close to the disk surface and touches the lubricant film, which often occurs due to externally given physical shock, are extremely important because it determines the consequence: recovery or fatal crash of the magnetic disk system.

Liquid molecules in the vicinity of a solid wall are captured by the potential of solid molecules, forming a layered structure.[1,2] This solidlike layered structure has been reported to show heat conduction properties similar to that of bulk liquids.[3] The layered structure, however, leads to a large influence on viscosity or resistance against stress as described below, and is also a significant influence on thermal phenomena via generation of thermal energy by shear and friction.

For a boundary lubrication system under the action of a constant frictional force, a stick-slip phenomenon is observed in which the sliding solid surface repeatedly sticks and slips. Its mechanism has been analyzed by taking into account the characteristics of the solidification of liquid molecules and fusion by shear.[4–6] As exemplified above, liquid in the vicinity of a solid-liquid interface exhibits a variety of flow characteristics depending on the conditions applied. An analysis of liquid flow by means of continuous fluid dynamics requires the appropriate boundary condition of liquid at the solid-liquid interface. The validity of the so-called no-slip condition commonly used has been discussed. A theory has been proposed[7] which claims that even when the no-slip condition holds for a microscopic solid-liquid interface, the boundary condition on the macroscopic scale can be regarded as a condition equivalent to slip. Such a virtual slip condition results from the fact that owing to the microscopic roughness of the interface, the liquid gains some freedom from confinement by the solid wall. In the experimental aspects, the stick of liquid molecules on a solid surface has been reported on the basis of measurements of flow rate and its driving forces for a system of slit flow,[8] while another experimental data have been reported suggesting the presence of slip at a solid-liquid interface[9] as well as the direct observation of slip.[10] Still another report has proposed that the presence of slip is dependent on the flow of liquid.[11] For a consistent elucidation of such phenomena, molecular dynamics simulation is very useful, and hence a number of computational experiments have been carried out.[12–25] In these simulations, the velocity distributions and shear stress

[a]Author to whom correspondence should be addressed. Fax: +81-22-217-5277. Electronic mail: ohara@ifs.tohoku.ac.jp

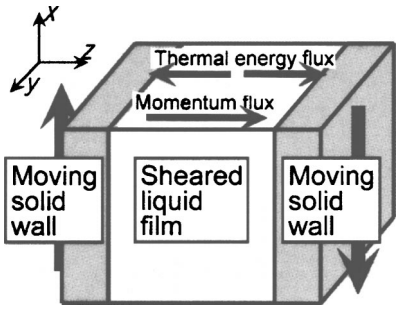

FIG. 1. Simulation system.

in the vicinity of the solid-liquid interface have been investigated for systems of Couette flow[12–24] or Poiseuille flow[12,13,25] of a liquid film interposed between two parallel solid walls. These studies have revealed the effects of various factors such as the number densities of solid and liquid molecules,[12,14–16] the strength of interaction between solid and liquid molecules,[12,14–21,25] the roughness of the solid surface,[16,22,23] the pressure of the system,[17] the gap between the solid walls,[13] and the molecular species of liquid.[20]

Fluid phenomena are accompanied by heat transfer phenomena because of the occurrence of viscous heating, as described above. From the viewpoint of thermal engineering, the thermal process is another important process, in which flow energy is converted to thermal energy and is transferred due to heat conduction from the liquid film to the solid walls via solid-liquid interfaces. In contrast to information about momentum transfer described above, little information is found in the literature about the generation and transfer of thermal energy in the liquid film and at solid-liquid interfaces. A review of previous work reveals only studies of thermal resistance at solid-liquid interfaces for a system composed of stationary liquid between solid walls at rest having different temperatures,[3,19,26–28] and studies of heat conduction and temperature distribution in Poiseuille flow[29] and Couette flow[24] between solid walls. In the above-mentioned studies[12–25] which aimed to discuss velocity distribution and momentum transfer in Poiseuille flow and Couette flow, some artificial treatments that may affect the generation and transfer of thermal energy were applied. For examples, solid walls which were not atomically structured and expressed by a time- and space-averaged potential,[13] adiabatic conditions for the solid wall were set by fixing solid molecules on their lattice position or assuming extremely large masses,[12,18,22,25] interaction among solid molecules was neglected,[14,15,17,19–21,23,24] and liquid temperatures were intentionally controlled.[13–16,18–21,23,25] These assumptions are not suitable for the analysis of thermal energy generation and transfer in the liquid-solid system. We have performed molecular dynamics simulations in which these points are taken into account, and analyzed the transfer of thermal energy and momentum in liquid films and at solid-liquid interfaces to reveal that a highly nonequilibrium state (unequal partition of thermal energy to each degree of freedom for molecular motion) exists in solid and liquid in the vicinity of the interface.[30,31]

The present study of liquid film sheared by solid walls focuses on the analysis of the thermal energy and momentum transfer at the solid-liquid interfaces and the effect of the crystal planes of the solid walls. The system modeled by the molecular dynamics simulations was composed of a liquid film with a thickness of the order of nanometers and solid walls placed on both sides of the liquid film. Thermal energy flux and momentum flux were generated simultaneously by applying shear to the liquid film by moving the solid walls in opposite directions, and characteristics of the energy and momentum transfer at the solid-liquid interface were examined. The present study suggests that these characteristics are influenced markedly by the structure of the crystal plane and the direction of shearing. The mechanism by which such a molecular scale structure influences the energy transfer at the interface was examined by analyzing the molecular motion and its contribution to energy transfer at the solid-liquid interface.

TABLE I. Solid walls employed in the simulation. The walls move along the *x* axis.

	Surface molecular number density	Surface crystal plane	Surface molecular configuration	Numbers of atoms in *x* and *y* directions	Numbers of layers in *z* direction
A	Largest	FCC (1,1,1)	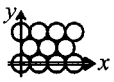	20×20	7
B	↑ ↓	FCC (1,0,0)	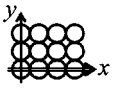	20×17	8
C	Small	FCC (1,1,0)	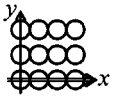	20×12	11
D				12×20	

II. SIMULATION SYSTEM AND METHOD

The simulation system used in the present study is shown in Fig. 1. The system is composed of two parallel solid walls and a thin liquid film imposed between the walls. Two isothermal solid walls were placed at both ends of the basic cell in the *z* direction, and the liquid film was sheared by moving the walls at a constant and identical rate (50 m/s or 100 m/s) in opposite directions along the *x* axis. As a result, macroscopic flow momentum was transferred along the *z* axis in the liquid film, being accompanied by a temperature rise due to viscous heating, and the thermal energy generated by the conversion of the flow energy was transferred due to heat conduction from the center region of the liquid film toward the solid walls. Periodic boundary conditions were applied in the *x* and *y* directions.

Four types of solid walls were modeled as shown in Table I. The solid walls were assumed to have a fcc structure. The crystal plane (111), (100), or (110) was in contact with the liquid. For the (110) plane, shearing in two directions was applied. These four types are named *A*–*D*, respectively. Each solid wall was constructed using 7–11 layers of solid

TABLE II. Parameters for the models of liquid molecules. Subscript "*LL*" and "*LS*" denote interaction between liquid molecules and that between liquid and solid molecules, respectively.

	Monatomic molecule	Linear molecule 1	Linear molecule 2
σ_{LL} (m)	3.41×10^{-10}	3.21×10^{-10}	3.41×10^{-10}
σ_{LS} (m)	3.09×10^{-10}	2.99×10^{-10}	3.09×10^{-10}
ε_{LL} (J)	1.67×10^{-21}	5.25×10^{-22}	1.67×10^{-21}
ε_{LS} (J)	1.67×10^{-21}	5.25×10^{-22}	1.67×10^{-21}
Site separation	⋯	$0.22\sigma_{\mathrm{LL}}$	$1.0\sigma_{\mathrm{LL}}$
Mass (at site) (kg)	6.63×10^{-26}	2.66×10^{-26}	6.63×10^{-26}

molecules in such a manner that the thickness in the *z* direction was almost identical for the four types of solid walls. No intentional control of molecular motion, such as temperature control, was applied in the calculation of molecular motion of solid and liquid molecules. However, the phantom molecules method[27] was applied so as to represent a heat bath at a constant temperature, to model an actual system that involves the part of a solid material (e.g., bearing) whose heat capacity is much larger than that of the liquid film. The phantom molecules are placed outside the solid molecule layers and excited by the random force of Gaussian distribution with a standard deviation whose magnitude is determined by the target temperature. The integrated interaction acting on the solid molecules from an isothermal semi-infinite solid is represented by the interaction between the solid molecules and the phantom molecules.

The interaction between solid molecules was modeled using a harmonic potential, with the potential parameters and mass values being those of platinum: the spring constant was 46.8 N/m, the equilibrium distance $r_{\mathrm{eq}}=2.77\times10^{-10}$ m, and the mass 3.24×10^{-25} kg. The dimensions of the basic cell in the *x* and *y* directions were fixed to ≈5.0 nm in every case by arranging 12–20 solid atoms in each direction.

A total of three types of liquid molecules were selected for simulation, a monatomic molecule and two types of linear molecules. The Lennard-Jones (12-6) potential corresponding to argon was used for the interaction between the monatomic molecules, and the two-center Lennard-Jones (LJ) potential was used for the linear molecules. The equation of state and thermal conductivity of fluids modeled by the two-center LJ potential have been studied in detail by Tokumasu *et al.*,[32] which guided us to select two sets of parameters for the linear molecules. The first species of linear molecule (molecule 1) is equivalent to an oxygen molecule, while the second species (molecule 2) is a hypothetic molecule which has a larger separation between the two sites than molecule 1, resulting in a larger contribution of rotational motion to heat conduction. The length parameter σ and energy parameter ε of these three types of molecules are collected in Table II. Here, subscripts "*LL*" and "*LS*" denote interaction between liquid molecules and that between liquid and solid molecules, respectively. The thickness of the liquid film, defined by the distance in the *z* direction between the time-averaged position of solid molecule layers, each of which contacted the liquid film at each end, was equated to $5\sigma_{LL}$ (several nanometers). The number of constituent molecules of the liquid film was determined by trial and error in such a way that the pressure of the liquid, which was measured by forces in the *z* direction acting on the solid walls, was within ±4 MPa so as not to influence the liquid structure. Interaction between a solid molecule and each site of a liquid molecule was modeled by the LJ potential; σ_{LS} was selected to be the mean of σ_{LL} and the equilibrium distance between solid molecules, and ε_{LS} was assumed to be equal to ε_{LL}. In all molecular dynamic simulations, every LJ potential was truncated at 5σ.

When the shear is applied to the liquid film, the temperature of the liquid film increases until it reaches a steady state at equilibrium. The value which the liquid film temperature reaches at the equilibrium is strongly dependent on the combination of the liquid molecule and the type of solid wall. In order to eliminate the effect of the difference between the liquid temperatures of the systems studied, the temperature of the phantom molecules in each system was selected in such a way that the average temperature of the layer of liquid molecules contacting the solid surface (referred to as the liquid contacting layer hereafter) at the equilibrium state was identical among the systems of the same liquid molecules with various walls and shear rates. The temperature of the liquid contacting layer mentioned here is based on the kinetic energy of liquid molecules due to the translational motion along the *z* axis (referred to as the *z* temperature hereafter), although thermal energy is not partitioned equally to all degrees of freedom for molecular motion, as will be described later, and the *x*, *y*, and *z* temperatures are not equal.

The average *z* temperature of the liquid contacting layer was selected to be 0.6–0.7 times the critical temperature[32] of the bulk liquid of each molecule: 110 K for the liquid of the monatomic molecule, 110 K for the linear molecule 1, and 140 K for the linear molecule 2.

The data for analyses were obtained by simulations with a time step of 2.5×10^{-15} s for 1 000 000 steps (for a system of the monatomic molecule liquid) or 2 000 000 steps (for systems of the linear molecules' liquid), after an equilibrium state was established by an equilibration run for the preceding 1 000 000 steps.

III. ANALYSIS OF THE SIMULATION RESULTS

Figure 2 shows examples of the number density distributions obtained by the simulation. Figure 2(a) displays the distribution for the combination of the linear molecule 2 and wall *A* with the velocity of ±100 m/s; the liquid molecules captured by the potential of the solid molecules form a layered structure parallel to the wall surface. The distribution peaks are broader and lower at positions more distant from the wall. Figure 2(b) compares the distributions for the combinations of molecule 2 with the four types of walls. Since every distribution is practically symmetrical about the center of the liquid film, the distribution curves are shown only in the region $0<z<2.5\sigma_{LL}$. The liquid contacting layer is at the furthest position from the wall in the case of wall *A*, the surface of which has the highest number density of mol-

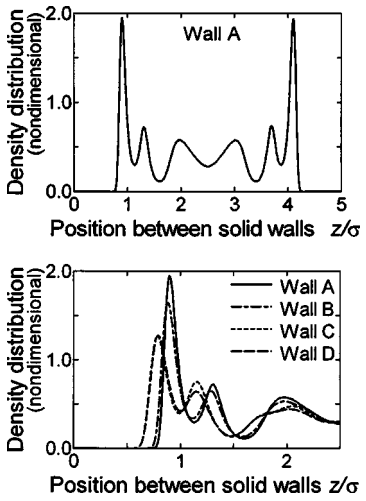

FIG. 2. Number density distribution of the center of mass of liquid molecules (linear molecule 2, velocity of the solid walls ±100 m/s). (a) The case with solid wall *A* over the whole range of liquid film (upper panel), (b) comparison between cases with walls *A*-*D* in the vicinity of the solid-liquid interface (lower panel).

ecules, and is closest to the wall in the cases of walls *C* and *D*, whose number densities are the lowest. The solid wall surface having a lower number density of molecules makes a potential surface with larger hollows, which capture liquid molecules. The peak of the liquid contacting layer is the highest for wall *A* and the lowest for walls *C* and *D*, in agreement with the relative number densities of solid molecules on the wall surfaces. The walls *C* and *D* have the same crystal plane and are different only in their shearing directions. The peaks of the contacting layer for walls *C* and *D* are almost identical, although some difference in the height of the second peaks exists at $z \sim 1.2\sigma_{LL}$ because of the difference in temperature at this position.

Figure 3 shows velocity and temperature distributions observed for the case of the linear molecule 2 and wall *A*.

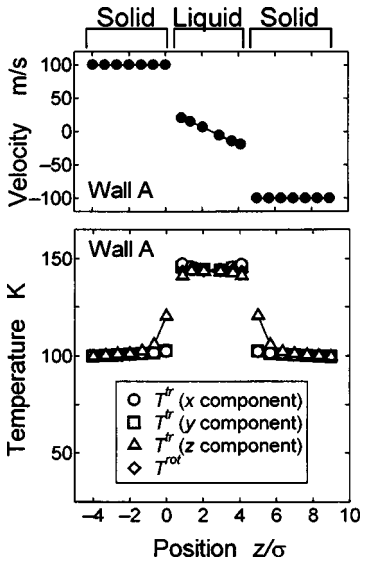

FIG. 3. Distributions of velocity (upper panel) and temperature (lower panel) in the liquid film and the solid walls (linear molecule 2, solid wall *A*, velocity of the solid walls ±100 m/s). Temperatures indicate thermal energy partitioned to each degree of freedom of molecular motion.

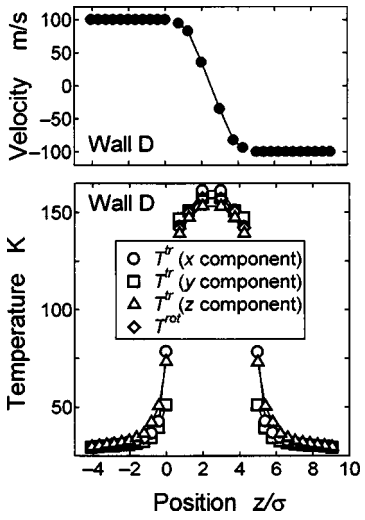

FIG. 4. Distributions of velocity (upper panel) and temperature (lower panel) in the liquid film and the solid walls (linear molecule 2, solid wall *D*, velocity of the solid walls ±100 m/s).

The averaged values over each layer of the solid and liquid molecules are plotted; seven data points on each side belong to the solid wall, and six points in the middle to the liquid film. Temperature T^{tr} was computed from the kinetic energy corresponding to each degree of freedom for molecular translational motion; the value for the *x* direction was based on the random component of velocity obtained by subtracting macroscopic Couette-like flow velocity. T^{rot} is a temperature computed from the rotational energy. Thus, the *x*, *y*, and *z* temperatures, $T_x^{\mathrm{tr}}, T_y^{\mathrm{tr}}, T_z^{\mathrm{tr}}$, respectively, and T^{rot} indicate how the thermal energy of the system is partitioned to each degree of freedom of molecular motion. Large jumps in temperature and velocity exist at the solid-liquid interfaces. The *x*-, *y*-, and *z*-temperature distributions in the solid and liquid exhibit significant differences among the degrees of freedom near the solid-liquid interfaces, which suggests that the energy is not equally partitioned among the degrees of freedom. The temperature distributions in the liquid film in the *x* and *y* directions have a shallow concave shape, and this form of the distribution is contrary to that predicted from macroscopic heat conduction concepts.

These features observed in the temperature and velocity distributions differ significantly according to the types of solid walls. Figure 4 shows the results of simulation for the case of wall *D* compared to Fig. 3 for the case with wall *A*. Although the temperature jump observed in Fig. 4 is larger than that for wall *A* in Fig. 3, the value of the thermal resistance is smaller because the heat conduction flux is much higher as shown in Fig. 5, which is a result of the high shear rate in the liquid. The inverse temperature gradient observed in Fig. 3 is not appreciable in this case. The velocity jump at the solid-liquid interface almost disappears, while a significant temperature jump still exits at the interface. This observation indicates that resistance at the interface acts differently on each of the transfers of thermal energy and momentum; in other words, there is a difference between transfer of thermal energy related to molecular motion of

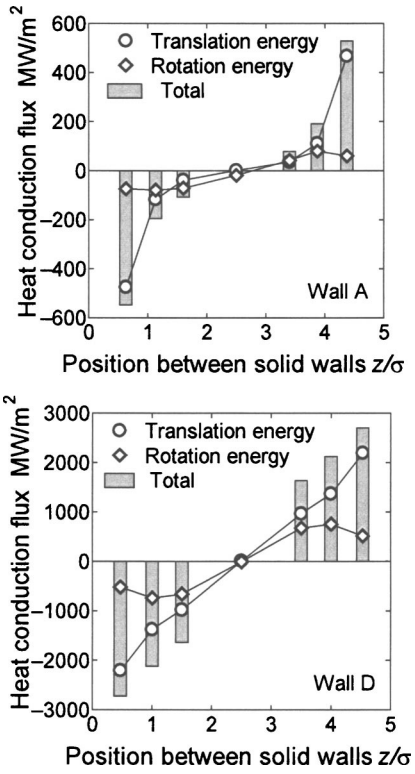

FIG. 5. Distribution of heat conduction flux and contributions of the translational and rotational energy transfer of molecules to the heat conduction flux observed in the liquid film and at the solid-liquid interfaces. The leftmost and rightmost plots are for the solid-liquid interfaces. [linear molecule 2, solid walls *A* (upper panel) and *D* (lower panel), velocity of the solid walls ±100 m/s].

various degrees of freedom and transfer of flow energy related to molecular motion of a specific degree of freedom.

The velocity distribution in the liquid film is almost linear, and the gradient is decreased in the vicinity of the walls. This is obvious in Fig. 4 for wall *D* and is present very slightly in Fig. 3 for wall *A*. This decrease in the gradient is due to a viscosity increase, which is caused by the layered structure of the liquid molecules in the vicinity of the solid walls.

All of the above characteristics found in Fig. 4 in case with wall velocity of ±100 m/s are observed also in case with wall velocity of ±50 m/s, where rate of liquid shear and viscous heating are similar to those in the case shown in Fig. 3.

The momentum flux and energy flux through a control surface S_{xy} are measured in the present system as follows. Regarding the momentum in the x direction: its flux in the z direction, P_{xz}, is given by[33]

$$P_{xz}S_{xy} = \sum_i (mv_{i,x}/1)\frac{v_{i,z}}{|v_{i,z}|} + \sum_i \sum_{j>i} F_{ij,x}\frac{z_{ij}}{|z_{ij}|}, \tag{1}$$

where m and v_i denote mass and velocity of molecule i, respectively. F_{ij} and z_{ij} are intermolecular forces between molecules i and j, and distance along the z axis between molecules i and j, respectively. The first term on the right side of Eq. (1) represents the transport of momentum of molecules themselves due to their motion; the summation is made over the molecules that pass through the control surface in a unit period of time. The second term represents the momentum transfer due to changes of molecular momentum caused by intermolecular forces acting between a pair of molecules; the double summation is made over all pairs of molecules which hold the control surface between them at a certain moment. In a similar way, the total energy flux in the z direction that passes through the control surface, $J_{\text{total},z}$, is given by[34]

$$J_{\text{total},z}S_{xy} = \sum_i \left[\left(\frac{1}{2}m\mathbf{v}_i^2 + \frac{1}{2}I\omega_i^2 + \phi_i\right)/1\right]\frac{v_{i,z}}{|z_{i,z}|} + \frac{1}{2}\sum_i \sum_{j>i} [\mathbf{F}_{ij}\cdot(\mathbf{v}_i + \mathbf{v}_j) + \mathbf{N}_{ij}\cdot\boldsymbol{\omega}_i - \mathbf{N}_{ji}\cdot\boldsymbol{\omega}_j]\frac{z_{ij}}{|z_{ij}|}, \tag{2}$$

where $\mathbf{F}$ and $\mathbf{v}$ are the vectors of intermolecular force and the velocity of molecules, respectively. $\mathbf{N}_{ij}$ and ω_i are the torque vector acting on molecule i due to its interaction with molecule j, and angular velocity vector of molecule i, respectively. In the second term of the right side of Eq. (2), $\mathbf{F}_{ij}\cdot(\mathbf{v}_i+\mathbf{v}_j)$ represents the contribution of the translational motion, which is referred to hereafter as translational energy transfer. The term $\mathbf{N}_{ij}\cdot\boldsymbol{\omega}_i - \mathbf{N}_{ji}\cdot\boldsymbol{\omega}_j$ is effective in cases of linear molecules only, which represents the contribution of the rotational motion, i.e., rotational energy transfer. The total energy flux given by Eq. (2) involves both the transfer of the macroscopic flow energy and the thermal energy. The thermal energy transfer, i.e., heat conduction flux, is obtained by using the random component of molecular velocity instead of the entire molecular velocity. The velocity vector $\mathbf{v}$ of a molecule is divided into the macroscopic flow velocity $\overline{\mathbf{v}}$ and the random component $\mathbf{v}'$, and substitution of $\mathbf{v}$ in Eq. (2) by $\mathbf{v}'$ gives the heat conduction flux $J_{\text{cond},z}$.

$$J_{\text{cond},z}S_{xy} = \sum_i \left[\left(\frac{1}{2}m\mathbf{v}_i'^2 + \frac{1}{2}I\omega_i^2 + \phi_i\right)/1\right]\frac{v_{i,z}}{|v_{i,z}|} + \frac{1}{2}\sum_i \sum_{j>i} [\mathbf{F}_{ij}\cdot(\mathbf{v}_i' + \mathbf{v}_j') + \mathbf{N}_{ij}\cdot\boldsymbol{\omega}_i - \mathbf{N}_{ji}\cdot\boldsymbol{\omega}_j]\frac{z_{ij}}{|z_{ij}|}. \tag{3}$$

In the present study, the control surfaces to measure the momentum flux and thermal energy flux were defined at the local minima in the number density distribution between layers of solid or liquid molecules, and at a position intermediate between the layers of solid and liquid molecules contacting each other across the solid-liquid interface. It is generally true in case of heat conduction in liquids that the second term on the right side of Eq. (3) associated with intermolecular interaction dominates over the first term. This tendency is promoted when the control surface is defined at the midpoint between the layers of liquid molecules. The present simulations have also shown that the contribution of the second term is 85%–95% of the total and is dominant in comparison with the first term. The second term is, therefore, analyzed in detail in the rest of this paper.

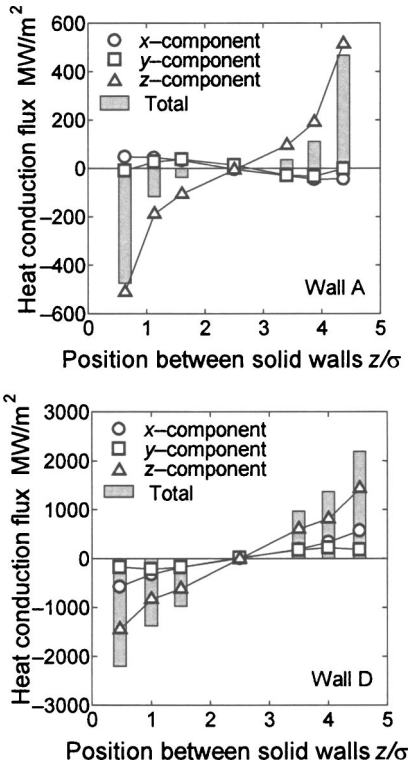

FIG. 6. Contributions of the molecular motions of each degree of freedom to the heat conduction flux due to translational motion of molecules observed in the liquid film and at the solid-liquid interfaces [linear molecule 2, solid walls *A* (upper panel) and *D* (lower panel), velocity of the solid walls ±100 m/s].

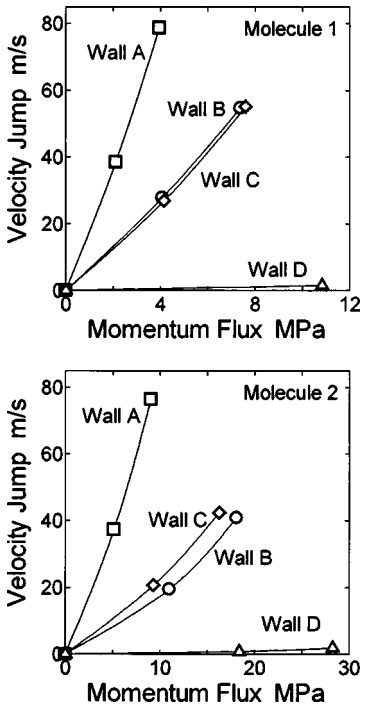

FIG. 7. Velocity jump vs momentum flux for the systems with the linear molecules 1 (upper panel) and 2 (lower panel).

Figure 5 shows the heat conduction flux, due only to the second term, measured at each control surface under the same simulation conditions as for Figs. 3 and 4. The heat conduction flux observed for the system with wall *D* is about five times as large as that with wall *A*, due to differences in the velocity gradients induced in the liquid film of the two systems. In Fig. 5, the translational energy transfer $\mathbf{F}_{ij}\cdot(\mathbf{v}_i+\mathbf{v}_j)$ and the rotational energy transfer $\mathbf{N}_{ij}\cdot\boldsymbol{\omega}_i-\mathbf{N}_{ji}\cdot\boldsymbol{\omega}_j$ are also plotted. The contribution of rotational energy transfer, which is about 30% in bulk liquid,[32] is larger than this value in the middle region of the liquid film, whereas it is much lower in the vicinity of the solid-liquid interface; this phenomenon is observed regardless of the type of solid wall.

Figure 6 shows the translational energy transfer plotted in Fig. 5, which is decomposed to the *x*, *y*, and *z* components in such a manner that $\mathbf{F}_{ij}\cdot\mathbf{v}_i=F_{ij,x}v_{i,x}+F_{ij,y}v_{i,y}+F_{ij,z}v_{i,z}$ and plotted in the figure. In the system with wall *A*, only the *z* component contributes to the translational energy transfer, while the *x* and *y* components make negative contributions, which is related to the inverse temperature gradient observed in Fig. 3. In contrast, in the system with wall *D*, the *x* and *y* components make positive contributions to the thermal energy transfer; this observation corresponds to the absence of an inverse temperature gradient in the liquid film as shown in Fig. 4. The contribution of the *x* component is larger than that of the *y* component, the mechanism of which will be discussed later.

Similar analyses were performed on the systems with walls *B* and *C*. The correlation between momentum flux and velocity jump at the solid-liquid interface, and that between heat flux and temperature jump, were examined for the cases of walls *A*–*D*.

To define the velocity jump at the solid-liquid interface, a velocity distribution curve for the Couette-like flow of liquid was approximated by a polynomial equation, and the flow velocity of the liquid at the solid-liquid interface was extrapolated using this equation. Here, the solid-liquid interface is assumed to be at a position that divides the distance between the averaged position of the layer of solid molecules and that of liquid molecules which contact each other with a ratio of $\sqrt[6]{2}\sigma_{LL}$ to r_{eq}. The velocity jump at the interface is defined as the difference between this liquid velocity at the interface and the velocity of the solid wall.

Velocity jumps thus obtained for a liquid film composed of the linear molecules 1 and 2 with the four types of solid walls are shown in Fig. 7 as functions of the momentum flux through the interface. The gradients of the curves increase with increasing momentum flux, which means that the momentum transfer characteristics between the solid wall and the liquid deteriorate at higher momentum flux and velocity jump. A similar behavior has been reported by Jabbarzadeh *et al.*[21] The ratio of velocity jump to momentum flux is, here, named momentum resistance in accordance with the concept of thermal resistance. For both cases with the linear molecules 1 and 2, wall *A* bears the highest momentum resistance, walls *B* and *C* have comparable values, and wall *D* has the lowest resistance; the value for wall *A* is 100–150 times as large as the value for *D*.

The characteristics obtained by a similar analysis for the liquid of the monatomic molecules, shown in Fig. 8, are somewhat different from those for the linear molecules. The difference between the cases with walls *B* and *C* has widened

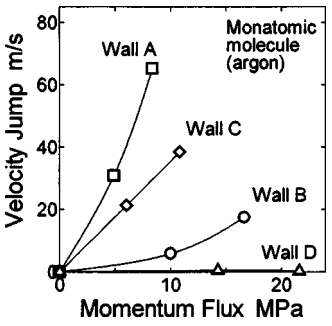

FIG. 8. Velocity jump vs momentum flux for the system with the monatomic molecule.

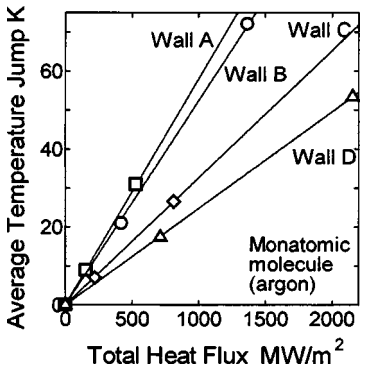

FIG. 9. Average temperature jump vs heat conduction flux (monatomic molecule).

and wall *C* is significantly more "slippery" than wall *B*, i.e., larger velocity jumps are needed to transfer momentum at the same rate. The momentum resistance increases in the order $D<B<C<A$. The difference between the cases with the linear molecules and the monatomic molecules is notable, although the linear molecule 1, which is equivalent to an oxygen molecule, is so short that its shape and potential surface are almost identical with those of the monatomic molecule. The detailed mechanism including the effect of molecular rotation should be clarified in future.

Commonly for the three types of liquid molecules, the wall *A* exhibits the largest momentum resistance, i.e., deteriorated momentum transfer characteristics. This phenomenon is thought to be associated with molecular-scale roughness of the potential surface made by the solid molecules at the solid-liquid interface. The surface of wall *A* has the highest molecular density, and hence has the smoothest potential surface in comparison with the other walls. The momentum resistances of walls *B*, *C*, and *D* are lower than that of wall *A*, supposedly because their more uneven potential surface enhances the exchange of momentum in the direction of shear between solid and liquid molecules. Wall *C* shows a higher momentum resistance than wall *D*, although they are composed of the same type of crystal plane. This observation indicates that a dominant factor for momentum resistance is the molecular-scale roughness of potential surface according to a positional change in the direction of shear, i.e., *x*.

Regarding the influence caused by the roughness of wall surface on slip at the solid-liquid interface, Jabbarzadeh *et al.*[23] assumed a system in which the wall had a sinusoidal surface and the liquid film consisted of polymer molecules with a length of about 5σ. Jabbarzadeh and co-workers examined the correlation between the period and amplitude of the sinusoidal roughness and the velocity jump at the solid-liquid interface. The influence of the period was notable in the range of $10\sigma-20\sigma$, and was not significant below 10σ. The present study has provided a new case that molecular scale roughness of crystal planes with a smaller period results in a marked influence on the velocity jump.

Concerning the correlation between the heat conduction flux and the temperature jump at the solid-liquid interface, no significant difference was observed among the species of liquid molecules examined in the present study. The correlation obtained for the case of the monatomic liquid molecules is shown in Fig. 9 as a typical result. The temperature jump is defined simply as the difference between the temperatures of the liquid- and solid-molecule layers contacting each other across the solid-liquid interface. The temperature jump has been determined for each of the *x*, *y*, and *z* temperatures, which do not coincide in the present case as was observed in Figs. 3 and 4, and the average of the three temperature jumps is shown in Fig. 9. Linear correlations between the temperature jump and the heat conduction flux are observed for the four types of walls. Thermal resistance, which is defined by the ratio of temperature jump to heat flux, corresponds to the gradient of the correlation line in the figure. As is observed in the figure, the resistances of walls *A* and *B* are comparable and are the largest, and wall *C* exhibits a larger resistance than wall *D*. This order does not agree with the orders shown in Figs. 7 and 8 for the momentum resistance. This disagreement is due to the fact that thermal energy transfer is caused by molecular motion of various degrees of freedom, while the momentum transfer is caused only by the molecular motion in the *x* direction, which will be discussed below.

Figure 10 shows the correlation for the system with monatomic liquid molecules and four types of solid walls, for which the temperature jump and the heat flux are decomposed to their *x*, *y*, and *z* components, and the correlations are plotted individually for each component. Here thermal resistance for each component is defined by the gradient of each straight line. As the main contribution to the heat flux is the *z* component, this component has the lowest thermal resistance. The negative gradients in the straight lines of the *x*

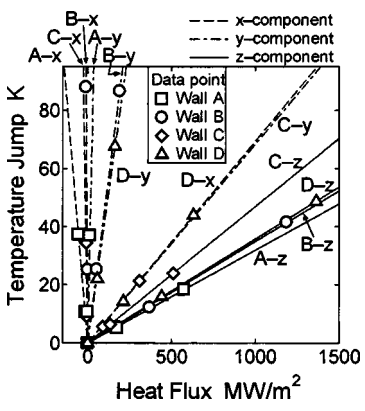

FIG. 10. Temperature jump vs heat conduction flux for each degree of freedom (monatomic molecule).

components for walls *A*, *B*, and *C* are caused by the negative thermal energy transfer of the *x* component, in a similar manner to those shown in Fig. 6 for the case of linear molecules.

The characteristics of the four types of solid walls appear in a different manner depending on the components. The *z* component that makes the largest contribution to the heat flux is associated with the molecular motion in the direction perpendicular to the solid-liquid interface, and hence the roughness of the potential surface of the solid wall is not an influencing factor, which is in contrast to the transfer of flow momentum. The major factor for the *z* component of heat flux is the number density of solid molecules on the wall surface, i.e., the number of molecules that can participate in the energy transfer. As a result, the *z* component of the thermal resistance is the lowest for wall *A* which has the highest surface number density of molecules, and then increases in the order $B<C$. The low thermal resistance for wall *D* may be related to the fact that other components of molecular motion also make a certain contribution to the thermal energy transfer and the energy of these components does not need to be converted to the *z* component before being transferred across the interface.

In contrast, the *x* and *y* components of the thermal energy transfer are strongly associated with the roughness of the potential surface of solid molecules, which liquid molecules experience according to a positional change in each of the *x* and *y* directions, even if the surface number density of solid molecules is lower to a certain extent as a sacrifice for the sake of the enhanced roughness. Consequently, walls *C* and *D* show the lowest thermal resistance for the *y* and *x* components, respectively. The thermal resistance for each of *x*, *y*, and *z* components is governed by those different factors, respectively, and the extent of the contribution of each component to the total heat flux is another factor to define the overall influence of the solid surface structure on the total thermal resistance shown in Fig. 9.

IV. CONCLUDING REMARKS

For a system composed of a pair of parallel solid walls and an ultrathin liquid film interposed between the walls, molecular dynamics simulation has been performed on the liquid film that is sheared by moving the walls. The thermal energy transfer and the transfer of macroscopic flow momentum at the solid-liquid interface have been analyzed, and the influence of the wall structure on the transfer characteristics has been examined. Fluxes of thermal energy and momentum, and the resulting jumps in temperature and velocity at the solid-liquid interface, have been measured for the combinations of four types of solid walls and three types of liquid molecules, and the dependence of the energy and momentum transfer characteristics on the type of solid wall have been elucidated. The results have revealed that certain components of energy and momentum transfer, which are due to the molecular motion in directions parallel to the solid-liquid interface, are governed by surface roughness at the molecular scale, i.e., the unevenness on the potential surface formed by the surface solid molecules that liquid molecules interact with as they move in the relevant direction. On the other hand, the component of energy transfer due to the molecular motion in the direction perpendicular to the surface, which is the major component of heat flux at the interface, is governed by the molecular number density on the solid surface.

The deviation from a macroscopic Couette flow is more notable at higher shearing rate. As the shearing rate is getting lower, the point in Figs. 7–9 approaches the origin of the figures, where the temperature and velocity jumps, and their differences among solid wall configurations diminish.

All of the results presented in this paper are derived using the same solid-liquid intermolecular potential for each liquid molecule. Although the present discussion on mechanism of energy transfer according to the degrees of freedom of molecular motion, and hence its qualitative difference among solid walls, are valid regardless of the epsilon, the magnitude of jumps in temperature and velocity will be sensitive to the epsilon. We are now doing more extensive parameter study to illustrate the entire view.

ACKNOWLEDGMENTS

This paper reports a portion of the work supported by the Grant-in-Aid for Scientific Research and the 21st Century COE Program "International COE of Flow Dynamics" by the Japan Society for the Promotion of Science (JSPS). All calculations were performed on a SGI Origin 2000 at the Advanced Fluid Information Research Center, Institute of Fluid Science, Tohoku University.

[1] P. C. Ball and R. Evans, Mol. Phys. **63**, 159 (1988).
[2] R. Kjellander and S. Sarman, Mol. Phys. **74**, 665 (1991).
[3] L. Xue, P. Keblinski, S. R. Phillpot, S. U.-S. Choi, and J. A. Eastman, Int. J. Heat Mass Transfer **47**, 4277 (2004).
[4] M. Schoen, C. L. Rhykerd, Jr., D. J. Diestler, and J. H. Cushman, Science **245**, 1223 (1989).
[5] P. A. Thompson and M. O. Robbins, Science **250**, 792 (1990).
[6] G. Reiter, A. L. Demirel, J. Peanasky, L. L. Cai, and S. Granick, J. Chem. Phys. **101**, 2606 (1994).
[7] S. Richardson, J. Fluid Mech. **59**, 707 (1973).
[8] D. Y. C. Chan and R. G. Horn, J. Chem. Phys. **83**, 5311 (1985).
[9] E. T. Watts, J. Krim, and A. Widom, Phys. Rev. B **41**, 3466 (1990).
[10] R. Pit, H. Hervet, and L. Leger, Phys. Rev. Lett. **85**, 980 (2000).
[11] Y. Zhu and S. Granick, Phys. Rev. Lett. **87**, 096105 (2001).
[12] J. Koplik, J. R. Banavar, and J. F. Willemsen, Phys. Fluids A **1**, 781 (1989).
[13] I. Bitsanis, S. A. Somers, H. T. Davis, and M. Tirrell, J. Chem. Phys. **93**, 3427 (1990).
[14] P. A. Thompson and M. O. Robbins, Phys. Rev. Lett. **63**, 766 (1989).
[15] P. A. Thompson and M. O. Robbins, Phys. Rev. A **41**, 6830 (1990).
[16] P. A. Thompson and S. M. Troian, Nature (London) **389**, 360 (1997).
[17] P. A. Thompson and G. S. Grest, Phys. Rev. Lett. **68**, 3448(1992).
[18] S. A. Somers and H. T. Davis, J. Chem. Phys. **96**, 5389 (1992).
[19] M. Cieplak, J. Koplik, and J. R. Banavar, Phys. Rev. Lett. **86**, 803 (2001).
[20] S. A. Gupta, H. D. Cochran, and P. T. Cummings, J. Chem. Phys. **107**, 10316 (1997).
[21] A. Jabbarzadeh, J. D. Atkinson, and R. I. Tanner, J. Non-Newtonian Fluid Mech. **69**, 169 (1997).
[22] J. Gao, W. D. Luedtke, and U. Landman, Tribol. Lett. **9**, 3 (2000).
[23] A. Jabbarzadeh, J. D. Atkinson, and R. I. Tanner, Phys. Rev. E **61**, 690 (2000).
[24] R. Khare, J. de Pablo, and A. Yethiraj, J. Chem. Phys. **107**, 2589 (1997).
[25] U. Heinbuch and J. Fischer, Phys. Rev. A **40**, 1144 (1989).
[26] L. Xue, P. Keblinski, S. R. Phillpot, S. U.-S. Choi, and J. A. Eastman, J. Chem. Phys. **118**, 337 (2003).
[27] S. Maruyama and T. Kimura, Therm. Sci. Eng. **7–1**, 63 (1999); S.

Maruyama, in *Advances in Numerical Heat Transfer*, edited by W. J. Minkowycz and E. M. Sparrow (Taylor & Francis, London, 2000, Vol. 2, Chap. 6, pp. 189–226.
[28]T. Ohara and D. Suzuki, Microscale Thermophys. Eng. **4**, 189 (2000).
[29]B. D. Todd and D. J. Evans, J. Chem. Phys. **103**, 9804 (1995).
[30]T. Ohara and T. Yatsunami, Microscale Thermophys. Eng. **7**, 1 (2003).
[31]T. Ohara and D. Torii, Microscale Thermophys. Eng. 9 (2005) (in print).
[32]T. Tokumasu, T. Ohara, and K. Kamijo, J. Chem. Phys. **118**, 3677 (2003).
[33]T. Ohara and D. Suzuki, Microscale Thermophys. Eng. **5**, 117 (2001).
[34]T. Ohara, J. Chem. Phys. **111**, 6492 (1999).